Pergamon

Tetrahedron 57 (2001) 3743–3752

TETRAHEDRON

Novel, terpyrrole-containing, aromatic expanded porphyrins

Jonathan L. Sessler,* Daniel Seidel, Christophe Bucher and Vincent Lynch

Department of Chemistry and Biochemistry, Institute for Cellular and Molecular Biology, The University of Texas at Austin, Austin, TX 78712-1167, USA

Received 18 October 2000; accepted 6 December 2000

Abstract—The synthesis and characterization of two expanded porphyrins, namely 18,23-diphenyl-2,3,6,7,10,11-hexamethyl-[26]hexaphyrin(1.1.1.1.0.0) and 18-mesityl-2,3,6,7,10,11-hexamethyl-[22]pentaphyrin(1.1.1.0.0) is described. Their common feature is a terpyrrolic subunit that is connected to a pyrrane building block. Both compounds display aromaticity and are stable in their respective protonated and free-base forms. © 2001 Elsevier Science Ltd. All rights reserved.

One of the most intriguing aspects of expanded porphyrin chemistry is the vast structural diversity that is seen within this general class of compounds.[1–3] While porphyrin itself is remarkably flexible, given its size, aromaticity, and pyrrole-based composition,[4] there are nonetheless limits to its ability to undergo conformational changes. On the other hand, expanded porphyrins with their attendant larger frameworks enjoy a greater conformational freedom. As a result, a range of structural motifs including 'figure eight' and other twisted forms, have been characterized in recent years.[1–3]

Over the course of the last two decades, considerable attention has been devoted to the synthesis of new oligopyrrolic systems. In spite of this progress, the factors that influence nonplanarity and conformational structure remain poorly understood. Particularly prominent in this context is the role of aromaticity. Here, one of the complicating factors is that, in contrast to what is true for porphyrins, many expanded porphyrins are nonaromatic or even formally antiaromatic. Further compounding the problem is the fact that for all conjugated polypyrrolic macrocycles, numerous oxidation states can be considered, the large majority of which contain either $(4n+2)$ π-electron or $4n$ π-electron peripheries. Finally, as a result of deviations from planarity, systems with either $(4n+2)$ or $4n$ π-electron peripheries can become essentially nonaromatic, as judged from their respective ^{1}H NMR spectral characteristics. This is true for systems such as turcasarin ([40]decaphyrin-(1.0.1.0.0.1.0.1.0.0)),[5] [32]octaphyrin(1.0.1.0.1.0.1.0),[6] [36]octaphyrin(2.1.0.1.2.1.0.1][7] and [34]octaphyrin-(1.1.1.0.1.1.1.0),[7] macrocycles that have shown to exhibit 'figure eight' structures in the solid state and in solution. Another octapyrrolic macrocycle, namely [32]octaphyrin(1.0.0.0.1.0.0.0),[8] does not exhibit a figure eight type structure. It does, however, deviate strongly from planarity and is, therefore, best considered as being nonaromatic.

Recently, even larger oligopyrrolic macrocycles have been reported with topologies that are anything but planar.[9,10] However, one requirement of aromaticity (and antiaromaticity as well) is 'some' degree of planarity.[11] Curiously, no macrocyclic system possessing more than six pyrrolic units is known that displays aromatic character. Indeed, in spite of its planarity, [28]heptaphyrin(1.0.0.1.0.0.0) (**1**), the first heptaphyrin to be reported in literature,[8] was found to be stable as an antiaromatic system, rather than as an aromatic one. In fact, many expanded porphyrins containing only five or six pyrrolic subunits are not aromatic.[1–3] In many instances this is because highly nonplanar conformations are adopted, with rosarin **2** (systematically: [24]hexaphyrin(1.0.1.0.1.0)) representing an extreme example of such behavior.[12,13]

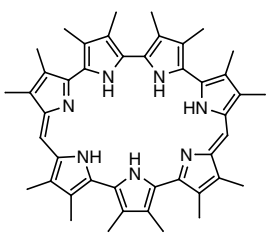

1

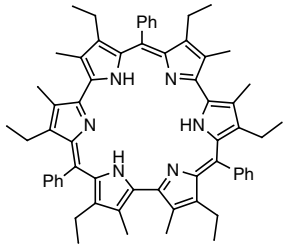

2

Quite recently, expanded porphyrins capable of achieving a planar arrangement by virtue of having one or two pyrrolic subunits 'inverted' (i.e. with their NH moieties 'flipped out') have been reported. One of the first systems of this type to be analyzed in detail is tetraphenylsapphyrin (**3**).

Keywords: macrocycles; porphyrin; aromaticity.

* Corresponding author. Tel.: +1-512-471-5009; fax: +1-512-471-7550; e-mail: sessler@mail.utexas.edu

PII: S0040-4020(01)00243-5

While inverted in the free base form, upon protonation, this macrocycle undergoes a conformational change to adopt a 'normal' structure with all five nitrogens pointing inward.[14,15] More recently, structural evidence was put forward in support of the contention that hexaphyrin **4** exhibits a bis-inverted structure.[16] Interestingly, the original hexaphyrin (**5**), reported by Gossauer in 1983,[17] was suggested as adopting a different conformation wherein the two *meso*-C*H* protons are pointing towards the cavity. This proposal, which would not require the inversion of pyrrolic subunits bearing large substituents (R=$CH_2CH_2CO_2CH_3$ for **5**) would nonetheless provide for an overall planar structure that displays typical aromatic features, as is indeed seen by experiment. By contrast, inversion is seen in the case of so-called heteroatom analogues of rubyrin, [26]hexaphyrin(1.1.0.1.1.0). While rubyrin **6** itself, synthesized with all β-pyrrolic positions substituted, yielded a solid state structure for its stable bis-protonated form with all six nitrogens pointing inward,[18] heterorubyrins (e.g. **7** with X=S or Se, respectively) display bis-inverted conformations under appropriate conditions.[19] Another mode of inversion has also been reported very recently.[20] It involves dioxarubyrin **8**, a system wherein two pyrroles within a bipyrrolic subunit are inverted.

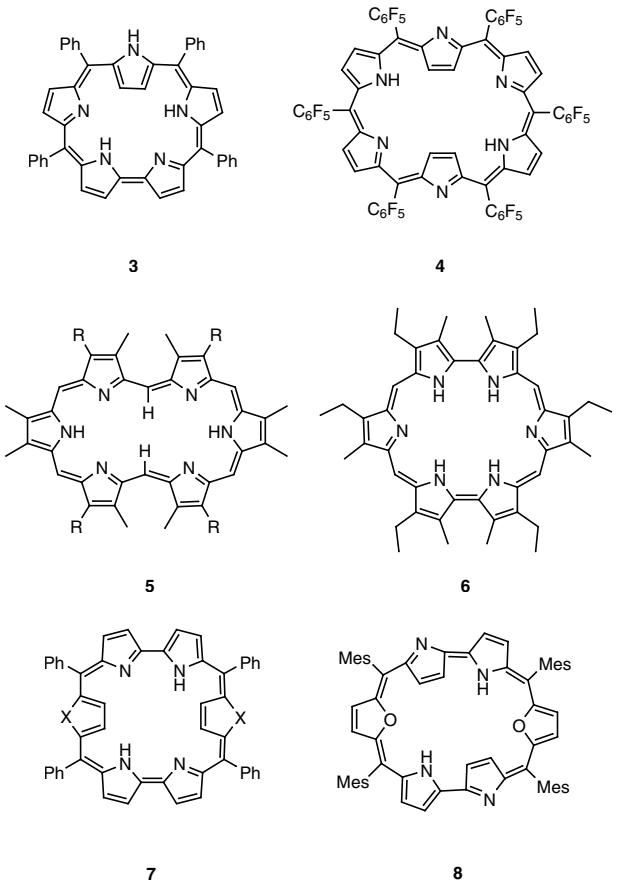

Given the fact that the large majority of macrocyclic systems containing inverted pyrrolic subunits have been obtained as the result of serendipity, rather than rational design, we became intrigued by the question of whether it would be possible to create a system that would be 'inverted' at a particular, pre-chosen pyrrolic site. Here, we reasoned that assembly of an expanded porphyrin-type macrocycle, wherein some of the pyrrolic subunits are β-substituted while others are not, might allow this goal to be attained. As detailed in a recent communication,[21] [26]hexaphyrin(1.1.1.1.0.0) (**11**), prepared in accord with such a strategy does indeed display pyrrole inversion at one specific and fully anticipated site.[21] Here, we wish to report full experimental details for this new expanded porphyrin, including further experimental support for the proposed inverted structure. We also report the successful synthesis of its smaller analogue, [22]pentaphyrin(1.1.1.0.0) (**14**). Both, **11** and **14** contain a terpyrrolic subunit incorporated within their macrocyclic frameworks. In both cases, these fragments are then 'fleshed out' with oligopyrrane fragments, tripyrrane or dipyromethane, respectively, that, in turn, were obtained from the condensation of pyrrole with benzaldehyde under appropriate conditions.[22,23]

As previously communicated[21] and as outlined in Scheme 1, [26]hexaphyrin(1.1.1.1.0.0) (**11**) is obtained from the acid catalyzed condensation of a 1:1 mixture of the diphenyltripyrrane **9** with the diformylhexamethylterpyrrole **10**. Carrying out this condensation in ethanol under conditions of reflux in the presence of air and an excess of *para*-toluenesulfonic acid (4 M equiv.), followed by chromatographic workup and treatment with NaOH, provides **11** in 46% yield as the sole isolable product.

The above success then led us to attempt the synthesis of [22]pentaphyrin(1.1.1.0.0) (**14a**). This smaller analog of **11** and an isomer of smaragdyrin, has recently been reported, but only in a form wherein all the β-pyrrolic sites of the macrocycle are substituted with alkyl groups.[24] By using a dipyrromethane with pyrroles that lack substituents in the β-positions, we intended to study whether this particular pentapyrrolic macrocycle, like its hexapyrrolic congener **11**, would be capable of undergoing inversion at one of its pyrrolic sites, presumably one of the less sterically demanding β-unsubstituted pyrroles. To the extent, this was found to occur, it would support the contention that the all β-substituted version, only characterized in the form of its HCl salt, would not be able to undergo such an inversion presumably as the result of [22]pentaphyrin(1.1.1.0.0) being unable to accommodate inward pointing alkyl groups.

Initial efforts to obtain [22]pentaphyrin(1.1.1.0.0) (**14a**) were made using a synthetic procedure analogous to that used to prepare **11**. Specifically, a mixture of diformylhexamethylterpyrrole, **13**[25] 5-phenyldipyrromethane, **12**[26] and 4 equiv. of *para*-toluenesulfonic acid was heated at reflux in ethanol for a period of 12 h while being left open

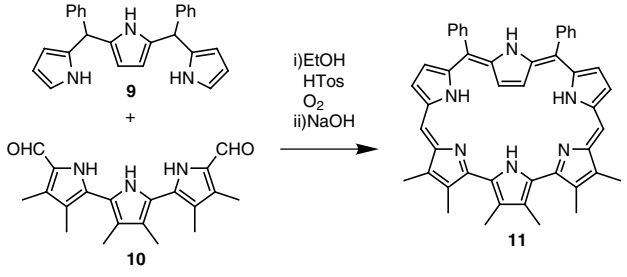

Scheme 1.

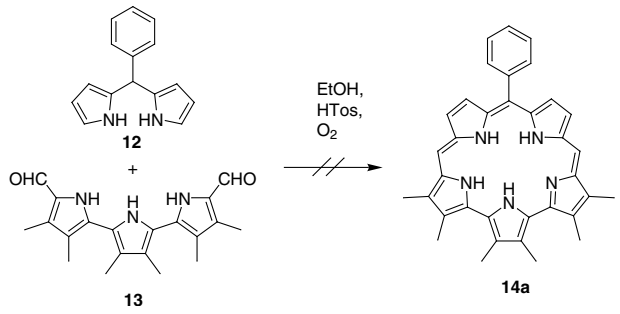

Scheme 2.

to the air. To our surprise, however, we were unable to isolate any of the desired products under these reaction conditions (Scheme 2). Accordingly, the approach and conditions used successfully to synthesize the all-β-substituted version of [22]pentaphyrin(1.1.1.0.0) were employed. Specifically, as outlined in Scheme 3, 1,9-bisformyl-5-phenyldipyrromethane (**15a**),[27] hexamethylterpyrrole (**16**) and an excess of HCl were reacted under an inert atmosphere using chloroform as the solvent, followed by chromatographic workup. In this instance, the desired product, phenylisosmaragdyrin **14a**, could be isolated in 44% yield in the form of its HCl-salt (H**14a**$^{+}\cdot$Cl^{-}). Unfortunately, H**14a**$^{+}\cdot$Cl^{-} proved to be only poorly soluble in most common organic solvents, such as dichloromethane, chloroform, acetonitrile and methanol. This hampered efforts at characterization. However, in d_7-DMF, satisfactory ^{1}H NMR spectral data could be obtained for H**14a**$^{+}\cdot$Cl^{-} that are in agreement with the proposed structure. Additionally, single crystals of H**14a**$^{+}\cdot$Cl^{-} suitable for X-ray crystallographic characterization could be obtained by recrystallization from DMSO. The resulting structure is shown in Fig. 1.

As illustrated in the top portion of Fig. 1, the protonated macrocycle H**14a**$^{+}\cdot$Cl^{-} interacts with the chloride counteranion that is located above the mean pentaaza plane. There are three hydrogen bonding interactions, namely between N5H–Cl (2.33(2) Å), N4H–Cl (2.28(2) Å) and N2H–Cl (2.46(2) Å). Two molecules of dimethylsulfoxide per macrocyclic unit are incorporated into the structure, only one of which is hydrogen bound to the macrocycle (cf. side view given in Fig. 1). There are two hydrogen bonding interactions involving this latter DMSO molecule, namely N1H–O (2.15(2) Å) and N3H–O (2.04(3) Å).

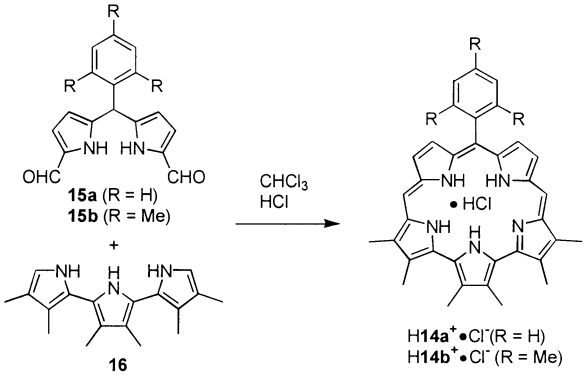

Scheme 3.

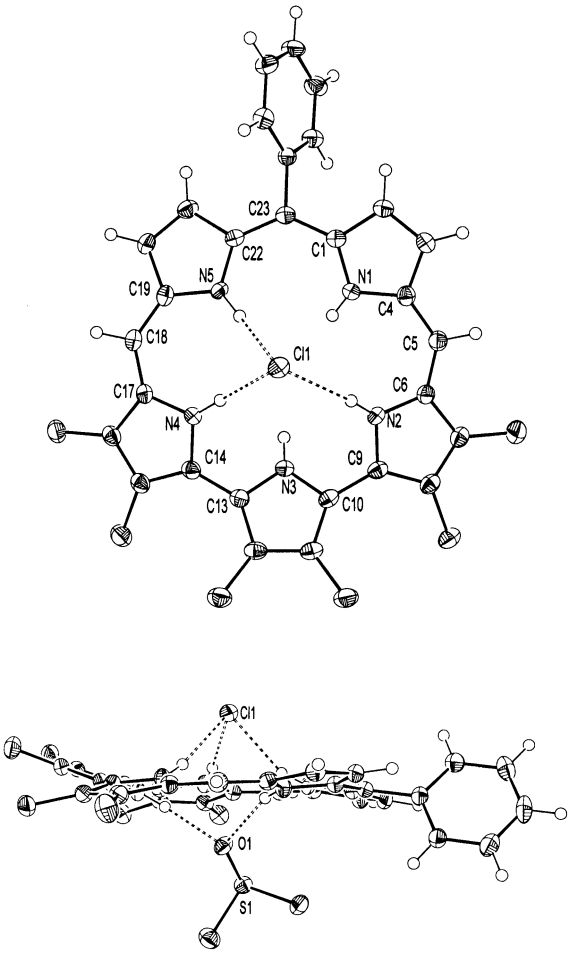

Figure 1. ORTEP[29] views of H**14a**$^{+}\cdot$Cl$^{-}\cdot$2DMSO showing a partial atom labeling scheme. The hydrogen atoms on the methyl groups have been omitted for clarity. Of the two DMSO molecules found in the structure, only one is shown in the side view of H**14a**$^{+}\cdot$Cl$^{-}\cdot$2DMSO. Dashed lines are indicative of a hydrogen bonding interaction. Thermal ellipsoids are scaled to the 50% probability level. Hydrogen atoms shown are drawn to an arbitrary scale.

On the basis of its proposed structure, H**14a**$^{+}\cdot$Cl^{-} is expected to be a $(4n+2)$ π-electron system and hence potentially aromatic. Nonetheless, the angles across the *meso* positions deviate substantially from 120°; they amount to 133.1 (C17–C18–C19), 131.4 (C22–C23–C1) and 132.1° (C4–C5–C6), respectively, indicating that the molecule experiences a severe strain. In spite of this, the overall molecule is rather planar as would be expected for an aromatic system. The main deviation from planarity involves the middle pyrrole of the terpyrrolic subunit, as indicated by torsion angles of 20.9 and 22.3° for N2–C9–C10–N3 and N3–C13–C14–N4, respectively. On the other hand, the dipyrromethane subunit is rather planar, with torsion angels of 3.2 (N5–C22–C23–C1) and 12.8° (C22–C23–C1–N1) being observed.

The structure of H**14a**$^{+}\cdot$Cl^{-} can be compared to that of H_2**11**$^{2+}\cdot$2Cl^{-} which was previously reported.[21] In this latter instance, pyrrole inversion, something not seen for H**14a**$^{+}\cdot$Cl^{-}, is observed. This leads to the conclusion that removal of alkyl groups in [22]pentaphyrin(1.1.1.0.0) is not, in and of itself, sufficient to induce pyrrole inversion, at least

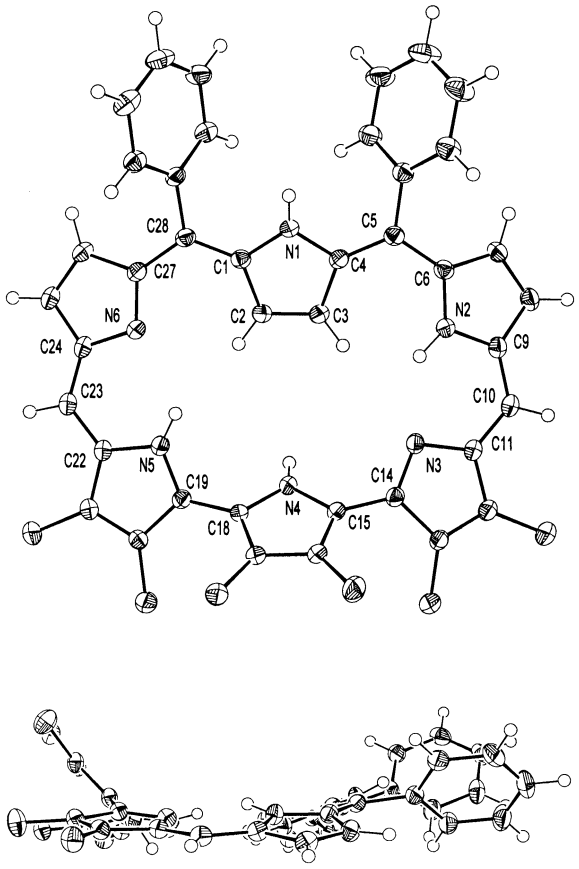

Figure 2. ORTEP[29] views of **11** showing a partial atom labeling scheme. The hydrogen atoms on the methyl groups have been omitted for clarity. Thermal ellipsoids are scaled to the 50% probability level. Hydrogen atoms shown are drawn to an arbitrary scale.

not at this protonation state and under these solid phase conditions. Accordingly, other protonation states were studied, not just in the case of **14a** but also **11**. In fact, in the course of the present study, we explicitly succeeded in growing X-ray diffraction quality single crystals of **11**. This aspect of the chemistry is discussed immediately below.

The free base form of [26]hexaphyrin(1.1.1.1.0.0) (**11**) was obtained by washing a chloroform solution of $H_2\mathbf{11}^{2+}\cdot 2Cl^-$ with aqueous NaOH. Single crystals were obtained from dichloromethane/hexanes. The resulting X-ray structure is depicted in Fig. 2. One feature of this structure is that **11** crystallizes under these conditions without any additional solvent being incorporated into the structure, in contradiction to what is commonly seen for similar systems (including $H_2\mathbf{11}^{2+}\cdot 2Cl^-$) that readily incorporate hydrogen bound and/or 'gap-filling' solvent molecules into their crystal lattices. The structure of **11** further deviates from that of $H_2\mathbf{11}^{2+}\cdot 2Cl^-$ in that a greater degree of distortion for the middle pyrrole of the terpyrrole subunit is seen in the free base form (cf. Table 1 for a detailed comparison of structural parameters). This latter subunit is tilted out of the plane in both instances; however, this distortion is greater for the free base form. This might explain the reduced ring current effect previously observed for **11** as compared to $H_2\mathbf{11}^{2+}\cdot 2Cl^-$.[21] On the other hand, the overall deviation from planarity for the tripyrrane subunit is less in the case of **11** than it was in the case of $H_2\mathbf{11}^{2+}\cdot 2Cl^-$.

Table 1. Solid state structural parameters for [26]hexaphyrin(1.1.1.1.0.0) **11** and its bis HCl salt, $H_2\mathbf{11}^{2+}\cdot 2Cl^-$

	11	$H_2\mathbf{11}^{2+}\cdot 2Cl^-$ [a]
Angles (°)		
C22–C23–C24	126.0	133.4
C27–C28–C1	122.2	120.9
C4–C5–C6	121.7	119.8
C9–C10–C11	126.4	132.7
Torsion angles (°)		
N3–C14–C15–N4	46.0	41.3
N4–C18–C19–N5	46.5	34.1
N6–C27–C1–C2	19.5	16.8
C27–C28–C1–C2	5.1	16.8
C3–C4–C5–C6	9.6	15.5
C4–C5–C6–N2	17.5	20.6

[a] Data taken from Ref. 21.

In order to obtain a more soluble version of [22]pentaphyrin(1.1.1.0.0) ($H\mathbf{14a}^+\cdot Cl^-$), we decided to replace the *meso*-phenyl group by a *meso*-mesityl group; it was hoped that such a replacement would serve to break up the various π-stacking interactions thought to account for the low solubility of the macrocycle. The requisite 1,9-bisformyl-5-mesityldipyrromethane (**15b**) was obtained from 5-mesityldipyrromethane using the common Vilsmeier-type conditions employed recently in the synthesis of 1,9-bisformyl-5-phenyldipyrromethane (**15a**).[27] With **15b** in hand, mesityl-isosmaragdyrin ($H\mathbf{14b}^+\cdot Cl^-$) could readily be obtained in 38% yield, using the same procedure used to prepare $H\mathbf{14a}^+\cdot Cl^-$. As expected, the solubility of $H\mathbf{14b}^+\cdot Cl^-$ improved as compared to $H\mathbf{14a}^+\cdot Cl^-$, with moderate solubility being observed in chloroform and dichloromethane. On the other hand, the solubility in DMSO was found to be reduced. The solubilities are similar for both the HCl-salt ($H\mathbf{14b}^+\cdot Cl^-$) and the free base form (**14b**), the latter being obtained upon treatment of $H\mathbf{14b}^+\cdot Cl^-$ with aqueous NaOH.

The UV–Vis spectra of $H\mathbf{14b}^+\cdot Cl^-$ and **14b** are shown in Fig. 3. The free base **14b** displays three strong absorptions, namely at 391, 458 and 473 nm, that are considered to be

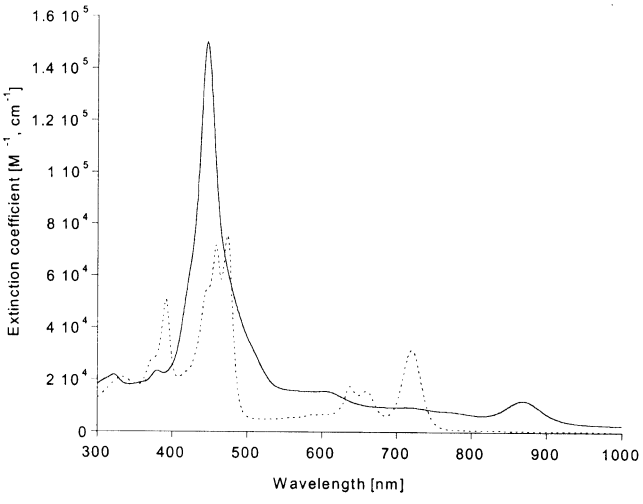

Figure 3. UV–Vis spectra of $H\mathbf{14b}^+\cdot Cl^-$ (—) and **14b** (- - -) recorded in dichloromethane.

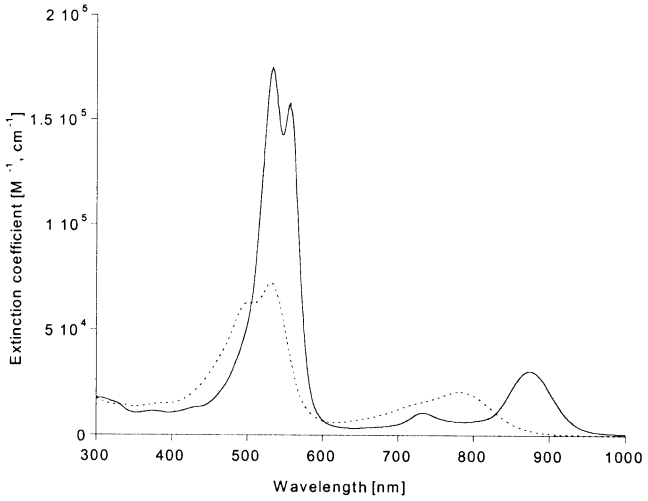

Figure 4. UV–Vis spectra of H_2**11**$^{2+}\cdot 2Cl^-$ (—) and **11** (- - -) recorded in dichloromethane.

Soret-type bands. Three weaker Q-like bands at 638, 659 and 720 nm are also observed. The UV–Vis spectrum of H**14b**$^+\cdot Cl^-$ is less complex and is characterized by a molar absorbtivity that is approximately twice as large as that of **14b**. Specifically, one sharp Soret-type band is seen at 447 nm and a single, less intense Q-type band is seen at 868 nm.

To facilitate comparisons, the UV–Vis spectra of **11** and H_2**11**$^{2+}\cdot 2Cl^-$ are displayed in Fig. 4. The spectra are in accord with what would be expected for a higher homologue of **14b**. For instance, analogous bands with similar extinction coefficients are seen in both series, with the bands for the larger hexapyrrolic system being red shifted as compared to the smaller macrocycle. For instance, a split Soret-type band at 502 and at 531 nm is seen for **11** (vs 391, 458 and 473 nm for **14**; vide supra). A single broad Q-type band at 782 nm is also observed for **11** (vs 638, 659 and 720 nm for **14b**). The UV–Vis spectrum of H_2**11**$^{2+}\cdot 2Cl^-$ is also characterized by a split Soret-like band at λ_{max} 533 and 556 nm and two Q-type transitions at 733 and 877 nm, respectively. Again, these are red shifted as compared to what is seen for H**14b**$^+\cdot Cl^-$. Such findings, taken in concert, are consistent with the proposal that all four species, **14**, **11**, H**14b**$^+\cdot Cl^-$ and H_2**11**$^{2+}\cdot 2Cl^-$ are aromatic and that the conjugation pathways in **11** and H_2**11**$^{2+}\cdot 2Cl^-$ are larger than in their pentapyrrolic congeners.

Further evidence that the new macrocyclic system **14b** is best considered as being aromatic came from ^{1}H NMR spectral studies. For instance, in the case of the free base **14b**, the ^{1}H NMR ($CDCl_3$) spectrum reveals signals at 3.71, 3.79 and 3.90 ppm, respectively, that are ascribed to the three different methyl groups attached to the β-pyrrolic positions. The downfield shifts of these resonances are typical of what is seen for alkyl groups attached to an aromatic periphery. Two doublets, corresponding to the β-pyrrole protons of the dipyrromethane subunit, are also seen at 8.78 and 9.49 ppm, respectively. The *meso*-like protons are found to resonate as one singlet at 10.38 ppm, in accord with what is expected based on symmetry considerations. The downfield position of this signal is indicative of an aromatic ring current effect. Unfortunately, in this instance, no resonances could be observed for another set of marker signals whose chemical shift values can provide evidence of aromaticity or antiaromaticity, namely the pyrrolic N*H* protons. Presumably, the inability to observe these latter signals reflects a fast equilibrium between different putative tautomers of the macrocycle. Consistent with such a supposition, it is interesting to note that the two *ortho*-methyl groups of the mesityl substituents are magnetically equivalent on the NMR time scale and therefore cannot be distinguished. They resonate as one singlet at 1.84 ppm. Since it appears reasonable to assume that the mesityl substituent is unable to rotate at room temperature, the observation of a singlet implies either a very flat overall macrocyclic structure or substantial conformational flexibility, with the result that the *ortho*-methyl groups of the mesityl substituent become chemically equivalent in a time average sense.[†]

The room temperature ^{1}H NMR spectrum ($CDCl_3$) of the protonated macrocycle H**14b**$^+\cdot Cl^-$ was also recorded and again found to be in accord with not only the proposed structure but also its ($4n+2$; $n=5$) π-electron aromatic formulation. For instance, the pyrrolic methyl groups were found to resonate between 3.75 and 3.84 ppm, while the expected doublets of the β-pyrrole protons of the dipyrromethane subunit were observed as two broad, unresolved singlets at 8.85 and 9.54 ppm, respectively. Another singlet at 10.53 ppm was also observed; it is ascribed to the two *meso*-like protons. Finally, in contrast to what proved true for the free base form of the macrocycle **14b**, all the expected N*H* resonances could be observed. Specifically, three singlets in the ratio of 1:2:2 and integrating to five protons were seen at −5.42, −2.84 and −2.11 ppm, respectively. Such upfield shifts for these signals are in accord with the proposed aromatic formulation and its attendant ring current effect.

Besides the observation of N*H* signals, one noteworthy difference between the ^{1}H NMR spectra of H**14b**$^+\cdot Cl^-$ and **14b** is that in the case of H**14b**$^+\cdot Cl^-$, the two *ortho*-methyl groups of the mesityl substituents give rise to two separate singlets at 1.59 and 2.14 ppm, respectively. This lack of equivalence provides support for the contention that not only is the mesityl group unable to rotate but also that the macrocyle as a whole is locked into a single conformation. Presumably, this is a consequence of interacting with, and binding to, the chloride counteranion; this, it is suggested, serves to stabilize in solution a structure analogous to that seen in the solid state (cf. Fig. 1), at least on the NMR time scale.

To date, in contrast to what is seen for the [26]hexaphyrin(1.1.1.1.0.0), system **11**, there has been no indication

[†] In an effort to 'visualize' the N*H* protons of **14b**, the spectrum was recorded in deuterated DMSO. Unfortunately, the very low solubility in this medium required acquisition times of two hours or longer in order to obtain a reasonable spectrum. Even under these conditions, a broadening of all signals was seen. In particular, no signals that could be ascribed to N*H* protons were observed, a finding consistent with strong interactions with solvent molecules. Increasing the temperature up to 80°C did not result in any significant sharpening of the various peaks and did not permit observation of the N*H* signals.

that either form of **14** (i.e. H**14b**$^{+}$·Cl^{-} or **14b**) displays any tendency to adopt a conformation in which one pyrrolic subunit is inverted. On the other hand, very interesting results were obtained when trifluoroacetic acid (TFA) was added stepwise to a solution of free base [22]pentaphyrin(1.1.1.0.0) (**14b**) in $CDCl_3$, including possible indications of pyrrole inversion at very high TFA concentrations.

At first, when less than one equivalent of trifluoroacetic acid is added to the solution, the ^{1}H NMR spectrum reflects the coexistence of both the free base and the protonated forms (**14b** and H**14b**$^{+}$·TFA^{-}). The addition of one full equivalent of trifluoroacetic acid then leads, as expected, to a disappearance of the signals ascribable to the free base form, and a growing in of spectral features ascribable to H**14b**$^{+}$·TFA^{-}. These latter, importantly, are virtually identical to those observed for H**14b**$^{+}$·Cl^{-}. Next, when a little bit more than one total equivalent of trifluoroacetic acid is added, extreme line broadening is observed. This is rationalized in terms of a fast exchange process involving binding and release of the TFA^{-} counteranion. This effect reaches its maximum at the point where a total of two equivalents of trifluoroacetic acid are added to the initial sample of **14b**. Indeed, at this juncture, practically no signals are observed. The addition of one further equivalent of trifluoroacetic acid (3 equiv. total) resulted in the observation of some peaks, albeit ones that remained extremely broad.

Once five or more equivalents (up to approximately 14 equiv.) of trifluoroacetic acid are added, a spectrum consistent with the formation of a new species is observed. On the basis of its NMR spectral features, this new species has been assigned the structure H_2**14b**$^{2+}$·2[TFA^{-}] (Scheme 4). Consistent with this assignment, all ^{1}H NMR chemical shifts are in accord with a nonaromatic system with little or no internal symmetry. For instance, six pyrrolic methyl signals are observed between 2.11 and 2.45 ppm, a region that implies that they are not experiencing any aromatic ring current effect. Five singlets between 10 and 13 ppm, whose chemical shift varies slightly depending on the precise amount of trifluoroacetic acid added, are also observed. These signals, ascribed to N*H* protons, resonate in a region that is very typical for 'normal' N*H* protons. Thus, this finding also supports strongly the proposed nonaromatic structure for H_2**14b**$^{2+}$·2[TFA^{-}]. Four doublets corresponding to the β-pyrrolic protons are also seen at 6.41, 6.66, 6.68 and 6.85 ppm. One of these latter (that at 6.41 ppm) was not resolved but was assigned as such based on a COSY spectral analysis. In any event, the chemical shift of these signals supports the contention that they do not experience any type of macrocyclic ring current effect.

In addition to the above, one singlet is found at 6.55 ppm. It integrates to one proton and is assigned to a *meso*-like C*H* resonance. Another singlet integrating to two protons and ascribed to a '*meso*'-CH_2-signal is also seen at 4.23 ppm. The presence of this CH_2-group is the result of a second protonation at the *meso* position, and accounts in large measure for the structure of H_2**14b**$^{2+}$·2[TFA^{-}] being assigned as depicted in Scheme 4. Still, in spite of this *meso* protonation, compound H_2**14b**$^{2+}$·2[TFA^{-}] appears flat (or time-averaged flat) as judged from the fact that the two *ortho*-methyl groups of the mesityl substituent are now magnetically equivalent; specifically, two singlets in the ratio of 2:1 are observed at 1.92 and 2.36 ppm, respectively. As expected, these signals show a crosspeak in the COSY spectrum.

When an even larger excess of trifluoroacetic acid is added (i.e. 100 M equiv. or more), the ^{1}H NMR spectrum changes again. Now, nine different methyl groups are observed, some of which are shifted to lower fields as compared to their presumed non-aromatic precursor H_2**14b**$^{2+}$·2[TFA^{-}]. The signal at 4.23 ppm that was ascribed to the '*meso*' CH_2 group in H_2**14b**$^{2+}$·2[TFA^{-}] is no longer present. On the other hand, one singlet integrating to one proton only, is observed at 8.2 ppm; it is assigned to a *meso*-C*H* proton. Four doublets, ascribed to the β-pyrrolic protons, are also observed. These latter signals are shifted downfield as compared to H_2**14b**$^{2+}$·2[TFA^{-}]. The best rationalization of these findings involves the generation of a species with an inverted '*meso*-carbon' such as **17**. For a species like this, one would expect to observe a signal for the inner *meso* C*H* proton that is shifted very far upfield as compared to the outer *meso*-C*H* proton. Unfortunately, however, a signal of this type could not be detected with any degree of certainty. Nor could signals corresponding to the N*H* protons be seen. While these signals may be hidden in the alkyl region, an inability to detect them unambiguously means that the structure assigned as **17** must be considered tentative as present.

The spectrum of **14b**+TFA gains further complexity when only slightly more trifluoroacetic acid is added to the

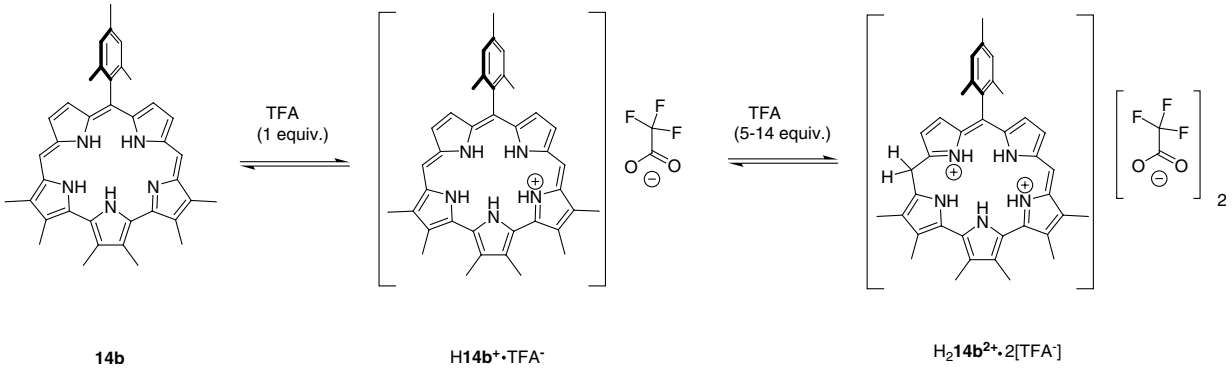

14b H**14b**$^{+}$·TFA^{-} H_2**14b**$^{2+}$·2[TFA^{-}]

Scheme 4.

solution in which **17** is considered to be the dominant species. This added complexity makes it extremely difficult to assign signals in the methyl region. Further, while the four doublets for the β-pyrrolic protons of **17** are seen to decrease in intensity, new signals are also seen to appear. These latter consist of two doublets at around 9.5 ppm and two doublets at approximately 5 ppm, all equal in intensity. While highly speculative at this stage of investigation, the presence of two sets of doublets, one shifted to higher field and one to lower field, is consistent with a structure such as **18** that has an inverted pyrrolic subunit. Given the rather small $\Delta\delta$ of the two sets of doublets, however, one would expect **18** to be highly distorted from planarity.

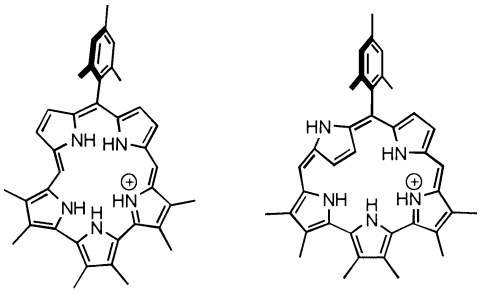

17 **18**

To shed further light on the changes seen upon varying the concentration of trifluoroacetic acid, we performed a UV–Vis titration starting with the free base **14b**. The results of this titration are summarized in Figs. 5 and 6, respectively. Fig. 5 shows the spectral changes presumed to occur during stepwise conversion of the free base **14b** to the monoprotonated species H**14b**$^{+}$·TFA^{-}, observed upon the addition of increasing quantities of TFA. Supporting the assumption of two species coexisting at equilibrium, an isosbestic point is observed over the course of this titration. Again, the final spectrum, assigned to H**14b**$^{+}$·TFA^{-}, is virtually identical to that of H**14b**$^{+}$·Cl^{-}.

The solution of H**14b**$^{+}$·TFA^{-} produced as the result of the above titration also provides the starting point for the addition of further trifluoroacetic acid, as shown in Fig. 6. Under the conditions of this second titration, the spectrum corresponding to H**14b**$^{+}$·TFA^{-} is seen to evolve gradually into a different one, specifically one considered to reflect the formation of the non-aromatic species H_2**14b**$^{2+}$·2[TFA^{-}]. In support of this latter conclusion is the finding that under these conditions, Q-type bands are no longer observed. Likewise, the intensity of the maximal Soret-like absorption is considerably decreased as compared to H**14b**$^{+}$·TFA^{-}. This latter band is also considerably broadened, a finding that is very much consistent with the presence of a nonaromatic species.

Fig. 7 shows the spectrum of **14b** measured in pure trifluoroacetic acid. This spectrum is clearly different from those assigned to H**14b**$^{+}$·TFA^{-} and H_2**14b**$^{2+}$·2[TFA^{-}]. In particular, it displays a small band around 700 nm that somewhat resembles a Q-type band. Such a band is, of course, expected were, as is being suggested, an aromatic species being formed at higher TFA concentrations. Unfortunately, these UV–Vis experiments, at least at their present level of

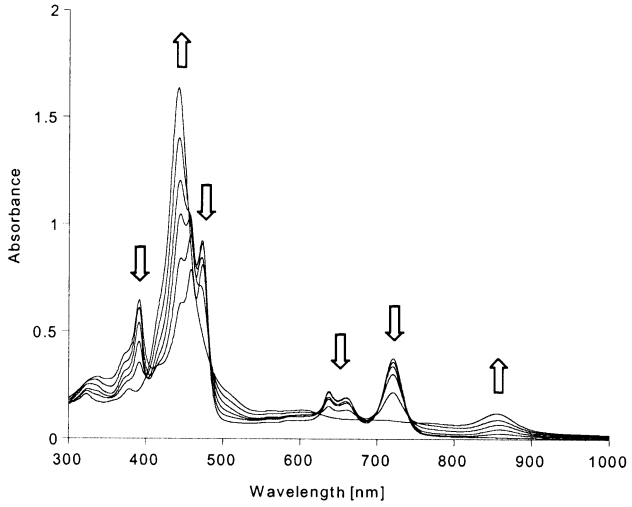

Figure 5. UV–Vis spectra showing the spectral changes observed upon the addition of TFA to solutions of **14b** in dichloromethane. These are considered to reflect the stepwise conversion of **14b** into H**14b**$^{+}$·TFA^{-}.

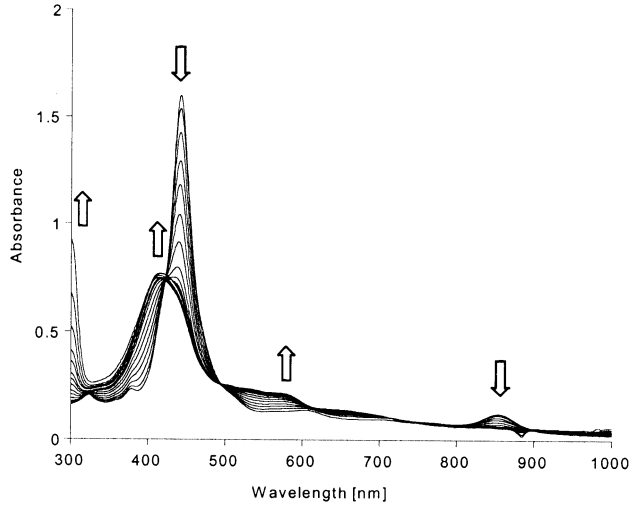

Figure 6. UV–Vis spectra showing spectral changes observed upon the addition of TFA to solutions of H**14b**$^{+}$·TFA^{-} in dichloromethane. These are considered to reflect the stepwise conversion of H**14b**$^{+}$·TFA^{-} into H_2**14b**$^{2+}$·2[TFA^{-}].

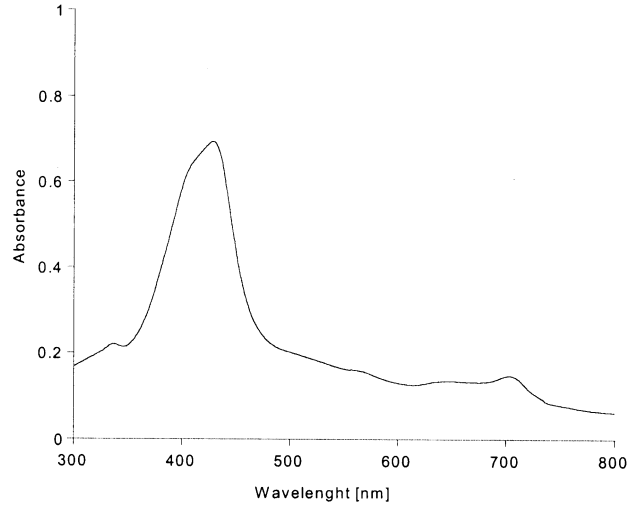

Figure 7. UV–Vis spectrum of **14b** in pure trifluoroacetic acid.

analysis, do not allow an assignment of whether pyrrole inversion has or has not occurred. On the other hand, they certainly do not rule it out.

In conclusion, the synthesis and characterization of the terpyrrole-derived pentapyrrolic and hexapyrrolic macrocycles **11** and **14**, containing aryl-substituted dipyrromethane and diaryl substituted tripyrrane subunits, respectively, have been described. The larger species display structures with an inverted pyrrole in both its free-base and diprotonated forms. By contrast, the smaller pentapyrrolic species **14** does not appear to contain an inverted pyrrole, at least in its well characterized free-base and monoprotonated forms. On the other hand, in the presence of excess trifluoroacetic acid, species are observed that, depending on the exact concentration of TFA, are either (i) non-conjugated (H_2**14b**$^{2+}\cdot 2[TFA^-]$) or (ii) aromatic with inverted '*meso*' carbons or (iii) pyrrolic subunits (**17** and **18**, respectively). While definite proof for the existence of these latter two structural variants (i.e. **17** and **18**) will require further study, the available data serves, at the very least, to underscore the fact that the protonation and conformational behavior of initially aromatic species such as **14b** is very complex.

1. Experimental

1.1. General

^{1}H and ^{13}C NMR spectra were measured at 25°C on a Varian Unity Plus spectrometer at 300 MHz, on a Varian Unity Innova at 500 MHz, or on a Bruker AC at 250 MHz. UV–Vis spectra were recorded on a Beckman DU-650 spectrophotometer. Low-resolution CI mass spectra were obtained on a Finnigan MATTSQ 700 mass spectrometer. High-resolution CI mass spectra were obtained on a VGZAB2-E mass spectrometer. All solvents and chemicals were obtained commercially and used as received.

1.1.1. 18,23-Diphenyl-2,3,6,7,10,11-hexamethyl-[26]hexaphyrin(1.1.1.1.0.0) (11). The tripyrrane **9** (56 mg 148 μmol) together with 50 mg (148 μmol) of the diformyl-terpyrrole **10** were suspended in 230 mL of ethanol. The resulting mixture was heated until complete dissolution of both components occurred. At this juncture, 120 mg (ca. 4 M equiv.) of *para*-toluenesulfonic acid was added, and the solution heated under reflux for an additional 12 h, open to air. After allowing the solution to cool to room temperature, the solvent was evaporated off under reduced pressure. The solid residue was dissolved in dichloromethane and subject to column chromatography, using silica gel as the stationary phase and dichloromethane (containing 5% methanol) as the eluent. The pink-red band was collected and the solvent removed under reduced pressure. The remaining solid was redissolved in 50 mL chloroform and washed with 1 M aqueous NaOH (2×10 mL). After drying the organic phase over anhydrous Na_2SO_4, removal of solvent in vacuo yielded 46 mg (46% yield) of **11** in the form of a dark microcrystalline powder. ^{1}H NMR (500 MHz, d_6-DMSO) δ [ppm] 2.11 (s, 6H, C*H*$_3$), 2.70 (s, 6H, C*H*$_3$), 2.84 (s, 6H, C*H*$_3$), 3.52 (d, J_{HH}=1.8 Hz, β-pyrrole C*H*), 7.26 (d, J_{HH}=4.2 Hz, 2H, β-pyrrole C*H*), 7.48 (m, 2H, phenyl-*H*), 7.67 (m, 4H, phenyl-*H*), 7.90 (bs, 4H, phenyl-*H*), 7.98 (d, J_{HH}=4.2 Hz, 2H, β-pyrrole C*H*), 8.53 (s, 2H, *meso-H*), 9.76 (s, 1H, N*H*); ^{13}C NMR (125 MHz, d_6-DMSO) δ [ppm] 10.48, 11.55, 11.86, 110.34, 114.6, 124.16, 125.48, 125.88, 126.66, 127.22, 128.55, 129.77, 132.27, 132.92, 134.37, 138.13, 138.97, 140.23, 143.16, 135.49; UV–Vis (CH_2Cl_2) λ_{max} [nm] (ε in $mol^{-1}\,L^{-1}$) 502 (61100), 531 (73400), 782 (20200); HRMS (CI): *m/z* 677.3399 (HM^+), calcd for $C_{46}H_{41}N_6$ 677.3393. H_2**11**$^{2+}\cdot 2Cl^-$ was obtained by washing a chloroform solution of **11** with 1 M aqueous HCl (2×10 mL). ^{1}H NMR (500 MHz, d_6-DMSO) δ [ppm] −1.99 (s, 2H, β-pyrrole C*H*), −0.75 (s, 1H, N*H*), −0.14 (s, 2H, N*H*), 0.05 (s, 2H, N*H*), 3.35 (s, 6H, C*H*$_3$), 3.73 (s, 6H, C*H*$_3$), 3.79 (s, 6H, C*H*$_3$), 7.89–7.92 (m, 2H, phenyl-*H*), 8.14–8.17 (m, 4H, phenyl-*H*), 8.93 (bs, 4H, phenyl-*H*), 9.17 (d, J_{HH}=4.3 Hz, 2H, β-pyrrole C*H*), 9.84 (d, J_{HH}=4.3 Hz, 2H, β-pyrrole C*H*), 11.35 (s, 2H, *meso-H*), 15.03 (s, 1H, N*H*); ^{13}C NMR (125 MHz, d_6-DMSO) δ [ppm] 12.16, 14.04, 14.77, 111.31, 112.34, 118.18, 123.37, 124.92, 125.46, 127.18, 128.52, 128.74, 129.31, 131.43, 131.50, 133.11, 135.43, 137.79, 139.73, 141.33, 144.54; UV–Vis (CH_2Cl_2) λ_{max} [nm] (ε in $mol^{-1}\,L^{-1}$) 533 (173000), 556 (156000), 733 (10400), 877 (30200).

1.1.2. 1,9-Bisformyl-5-mesityldipyrromethane (15b). In a 50 mL round bottom flask equipped with a reflux condenser and a septum, dry DMF (5 mL) was cooled with stirring for 10 min in an external ice water bath under argon. Freshly distilled $POCl_3$ (1 mL) was then added slowly via syringe. The ice bath was removed and the reaction mixture was stirred at room temperature for 20 min. The resulting yellow solution was cooled using an external ice water bath before addition of 1 g (3.78 mmol) of *meso*-(mesityl)dipyrromethane[28] dissolved in 10 mL of dry DMF. After addition, the reaction mixture was heated to 80°C for an hour. The resulting reddish mixture was then allowed to cool to room temperature at which point saturated aqueous NaOAc (30 mL) was added. The reaction mixture was reheated to 80°C for a period of 15 min and subsequently added to 300 mL of ice water. The solid, that precipitated out as the result of this addition was isolated by filtration and washed with water until the pH of the washings were neutral. Yield of **15b**: 0.9 g (74%). ^{1}H NMR (250 MHz, $CDCl_3$): δ [ppm] 2.04 (s, 6H), 2.26 (s, 3H), 5.93 (s, 1H), 6.09 (m, 2H), 6.86 (s, 2H), 6.88 (m, 2H), 9.23 (s, 2H), 9.55 (bs, 2H); ^{13}C NMR (62.5 MHz, $CDCl_3$): δ [ppm] 20.5, 20.7, 38.9, 110.9, 122.0, 130.4, 130.9, 132.0, 137.2, 137.5, 140.3, 178.1; HRMS (CI): *m/z* 321.1606, calcd for $C_{20}H_{20}N_2O_2$ $(M+1)^+$: 321.1603.

1.1.3. 18-Phenyl-2,3,6,7,10,11-hexamethyl-[22]pentaphyrin(1.1.1.0.0) (14a). In a 500 mL round bottom flask, 1,9-bisformyl-5-phenyldipyrromethane (**15a**)[27] (50 mg, 0.18 mmol) and hexamethylterpyrrole **16** (50.5 mg, 0.18 mmol) were dissolved in 300 mL of chloroform. Argon was bubbled through the resulting solution for about 15 min. Two drops of concentrated HCl in 2 mL of ethanol were then added and the reaction mixture stirred for 10 h while maintaining it under a positive argon atmosphere. The reaction vessel was then opened to the air and stirring was continued for an additional two hours. The solvent was then evaporated off under reduced pressure and the remaining was subjected to purification

via column chromatography (silica gel; 2% methanol in dichloromethane eluent). The green fractions were combined and the volume of solvent was reduced to approximately 20 mL, using a rotary evaporator. The resulting solution was placed in a fridge overnight, and the resulting green microcrystalline material was filtered off and washed with a small amount of dichloromethane. Drying under vacuum yielded 44 mg (44% yield) of H**14a**$^{+}\cdot Cl^{-}$. ^{1}H NMR (500 MHz, d$_7$-DMF) δ [ppm] −2.32 (bs, 3H, N*H*), −1.87 (bs, 2H, N*H*), 3.72 (s, 6H, CH_3), 3.78 (bs, 6H, CH_3), 3.87 (s, 6H, CH_3), 7.93 (bs, 3H, phenyl-*H*), 8.15–8.5 (bm, 2H, phenyl-*H*), 8.68 (bs, 2H, β-pyrrole-*H*), 9.75 (bs, 2H, β-pyrrole-*H*), 10.79 (bs, 2H, *meso-H*).

1.1.4. 18-Mesityl-2,3,6,7,10,11-hexamethyl-[22]pentaphyrin(1.1.1.0.0) (14b). Using a procedure identical to that described above, 1,9-bisformyl-5-mesityldipyrromethane (**15b**) (190 mg, 0.59 mmol) was condensed with hexamethylterpyrrole **16** (167 mg, 0.59 mmol) to produce **14b**. In this instance, chromatographic workup (silica gel; 0.5% methanol in dichloromethane, eluent) yielded the product as a green band. Collection and recrystallization from dichloromethane/hexanes then provided 135 mg (38% yield) of a green microcrystalline solid (H**14b**$^{+}\cdot Cl^{-}$). ^{1}H NMR NMR (300 MHz, $CDCl_3$) δ [ppm] −5.42 (bs, 1H, N*H*), −2.84 (bs, 2H, N*H*), −2.11 (bs, 2H, N*H*), 1.59 (s, 3H, mesityl-CH_3), 2.14 (s, 3H, mesityl-CH_3), 2.73 (s, 3H, mesityl-CH_3), 3.75 (s, 12H, pyrrole-CH_3), 3.84 (s, 6H, pyrrole-CH_3), 7.37 (s, 1H, mesityl-*H*), 7.47 (s, 1H, mesityl-*H*), 8.85 (bs, 2H, β-pyrrole-C*H*), 9.54 (bs, 2H, β-pyrrole-C*H*), 10.53 (bs, 2H, *meso*-C*H*); ^{13}C NMR (75 MHz, $CDCl_3$) δ [ppm] 12.15, 14.07, 14.41, 20.25, 21.53, 99.74, 102.86, 120.66, 121.75, 123.23, 124.65, 125.97, 126.86, 128.39, 130.21, 132.13, 137.49, 138.34, 141.31; HRMS (CI): *m/z* 601.2977 (M^+), calcd for $C_{38}H_{40}N_5Cl_1$ 601.2972, *m/z* 566.3282 (M^+-Cl), calcd for $C_{38}H_{40}N_5$ 566.3284; UV–Vis (CH_2Cl_2) λ_{max} [nm] (ϵ in $mol^{-1}\,L^{-1}$) 447 (150000), 868 (12000). The free base form, **14b**, was obtained by washing a CH_2Cl_2 solution of the corresponding HCl-salt H**14b**$^{+}\cdot Cl^{-}$ with 1 M aqueous NaOH (3×). Drying of the resulting solution over anhydrous Na_2SO_4 and concentration of the solution to a minimal volume on the rotary evaporator led to crystallization of the free base **14b** in the form of blue crystals, which were collected via vacuum filtration. ^{1}H NMR NMR (300 MHz, $CDCl_3$) δ [ppm] 1.84 (s, 6H, mesityl-CH_3), 2.70 (s, 3H, mesityl-CH_3), 3.71 (s, 6H, pyrrole-CH_3), 3.79 (s, 6H, pyrrole-CH_3), 3.90 (s, 6H, pyrrole-CH_3), 7.38 (s, 2H, mesityl-*H*), 8.78 (d, J_{HH}=4.5 Hz, 2H, β-pyrrole-C*H*), 9.49 (d, J_{HH}=4.5 Hz, 2H, β-pyrrole-C*H*), 10.38 (s, 2H, *meso*-C*H*); ^{13}C NMR (75 MHz, $CDCl_3$) δ [ppm] 12.12, 14.64, 21.03, 22.11, 30.93, 97.16, 101.27, 120.63, 121.49, 122.52, 124.60, 126.00, 126.58, 127.95, 129.82, 131.57, 131.99, 137.08, 138.21, 140.00; HRMS (CI): *m/z* 566.3286 (M^+), calcd for $C_{38}H_{40}N_5$ 566.3284; UV–Vis (CH_2Cl_2) λ_{max} [nm] (ϵ in $mol^{-1}\,L^{-1}$) 391 (50600), 458 (71600), 473 (75300), 638 (17500), 659 (15600), 720 (31600).

1.2. Nonaromatic species tentatively assigned as H_2**14b**$^{2+}\cdot$2[TFA^-]

^{1}H NMR (500 MHz, $CDCl_3$) δ [ppm] 1.92 (s, 6H, mesityl-CH_3), 2.11 (s, 3H, pyrrole-CH_3), 2.27 (s, 3H, pyrrole-CH_3), 2.30 (s, 3H, pyrrole-CH_3), 2.31 (s, 3H, pyrrole-CH_3), 2.36 (s, 3H, mesityl-CH_3), 2.42 (s, 3H, pyrrole-CH_3), 2.45 (s, 3H, pyrrole-CH_3), 4.23 (s, 2H, '*meso*'-CH_2) 6.41 (bs, 1H, β-pyrrole-C*H*), 6.55 (s, 1H, *meso-H*), 6.66 (d, J_{HH}=3.7 Hz, 1H, β-pyrrole-C*H*), 6.68 (d, 1H, J_{HH}=2.8 Hz, β-pyrrole-C*H*), 6.85 (d, J_{HH}=3.7 Hz, 1H, β-pyrrole-C*H*), 6.95 (s, 2H, mesityl-*H*), 10.05 (s, 1H, N*H*), 10.22 (s, 1H, N*H*), 10.67 (s, 1H, N*H*), 11.59 (s, 1H, N*H*), 12.11 (s, 1H, N*H*); ^{13}C NMR (125 MHz, $CDCl_3$, extracted from hmbc and hmqc projection) δ [ppm] 9.09, 9.84, 11.35, 12.28, 13.04, 19.05, 20.93, 25.81, 103.21, 119.37, 120.49, 121.62, 122.00, 124.63, 125.56, 126.50, 127.26, 128.38, 129.89, 130.07, 130.82, 131.58, 132.89, 133.83, 135.14, 137.96, 139.84, 143.22, 144.16, 145.85, 146.42, 147.73.

Acknowledgements

We are indebted to Dr Ben Shoulders, Steve Sorey and the staff at the NMR facility at the University of Texas for their assistance. This work was supported by the National Science Foundation (grant CHE-9725399 to J. L. S.).

References

1. Sessler, J. L.; Weghorn, S. J. *Expanded Contracted and Isomeric Porphyrins*, Vol. 15; Pergamon: New York, 1997.
2. Jasat, A.; Dolphin, D. *Chem. Rev.* **1997**, *97*, 2267–2340.
3. Sessler, J. L.; Gebauer, A.; Weghorn, S. J. Expanded Porphyrins. In *The Porphyrin Handbook*; Kadish, K. M., Smith, K. M., Guilard, R., Eds.; Academic: San Diego, 2000; vol. 2, pp 55–124.
4. Senge, M. O. Highly Substituted Porphyrins. In *The Porphyrin Handbook*; Kadish, K. M., Smith, K. M., Guilard, R., Eds.; Academic: San Diego, 2000; vol. 1, pp 239–347.
5. Sessler, J. L.; Weghorn, S. J.; Lynch, V.; Johnson, M. R. *Angew. Chem., Int. Ed. Engl.* **1994**, *33*, 1509–1512.
6. Bröring, M.; Jendrny, J.; Zander, L.; Schmickler, H.; Lex, J.; Wu, Y.-D.; Nendel, M.; Chen, J.; Plattner, D. A.; Houk, K. N.; Vogel, E. *Angew. Chem., Int. Ed. Engl.* **1995**, *34*, 2515–2517.
7. Vogel, E.; Bröring, M.; Fink, J.; Rosen, D.; Schmickler, H.; Lex, J.; Chan, K. W. K.; Wu, Y.-D.; Plattner, D. A.; Nendel, M.; Houk, K. N. *Angew. Chem., Int. Ed. Engl.* **1995**, *34*, 2511–2514.
8. Sessler, J. L.; Seidel, D.; Lynch, V. *J. Am. Chem. Soc.* **1999**, *121*, 11257–11258.
9. Setsune, J.-i.; Katakami, Y.; Iizuna, N. *J. Am. Chem. Soc.* **1999**, *121*, 8957–8958.
10. Lash, T. D. *Angew. Chem., Int. Ed. Engl.* **2000**, *39*, 1763–1767.
11. Minkin, V. I.; Glukhovtsev, M. N.; Simkin, B. Y. *Aromaticity and Antiaromaticity*, Wiley: New York, 1994.
12. Sessler, J. L.; Weghorn, S. J.; Morishima, T.; Rosingana, M.; Lynch, V.; Lee, V. *J. Am. Chem. Soc.* **1992**, *114*, 8306–8307.
13. Lament, B.; Dobkowski, J.; Sessler, J. L.; Weghorn, S. J.; Waluk, J. *Chem. Eur. J.* **1999**, *5*, 3039–3045.
14. Chmielewski, P. J.; Latos-Grazynski, L.; Rachlewicz, K. *Chem. Eur. J.* **1995**, *1*, 68–73.
15. Rachlewicz, K.; Sprutta, N.; Latos-Grazynski, L.; Chmielewski, P. J.; Szterenberg, L. *J. Chem. Soc., Perkin Trans. 2* **1998**, 959–967.
16. Neves, M. G. P. M. S.; Martins, R. M.; Tomé, A. C.; Silvestre,

A. J.; Silva, A. M. S.; Félix, V.; Drew, M. G. B.; Cavaleiro, J. A. S. *Chem. Commun.* **1999**, 385–386.
17. Gossauer, A. *Chimia* **1983**, *37*, 341–342.
18. Sessler, J. L.; Morishima, T.; Lynch, V. *Angew. Chem., Int. Ed. Engl.* **1991**, *30*, 977–980.
19. Narayanan, S. J.; Sridevi, B.; Chandrashekar, T. K.; Vij, A.; Roy, R. *J. Am. Chem. Soc.* **1999**, *121*, 9053–9068.
20. Narayanan, S. J.; Srinivasan, A.; Sridevi, B.; Chandrashekar, T. K.; Senge, M. O.; Sugiura, K.-i.; Sakata, Y. *Eur. J. Org. Chem.* **2000**, 2357–2360.
21. Sessler, J. L.; Seidel, D.; Bucher, C.; Lynch, V. *Chem. Commun.* **2000**, 1473–1474.
22. Brückner, C.; Sternberg, E. D.; Boyle, R. W.; Dolphin, D. *Chem. Commun.* **1997**, 1689–1690.
23. Bucher, C.; Seidel, D.; Lynch, V.; Král, V.; Sessler, J. L. *Org. Lett.* **2000**, *2*, 3103–3106.
24. Sessler, J. L.; Davis, J. M.; Lynch, V. *J. Org. Chem.* **1998**, *63*, 7062–7065.
25. Meyer, S.; Andrioletti, B.; Sessler, J. L.; Lynch, V. *J. Org. Chem.* **1998**, *63*, 6752–6756.
26. Lee, C.-H.; Lindsey, J. S. *Tetrahedron* **1994**, *50*, 11427–11440.
27. Clarke, O. J.; Boyle, R. W. *Tetrahedron Lett.* **1998**, *39*, 7167–7168.
28. Littler, B. J.; Miller, M. A.; Hung, C.-H.; Wagner, R. W.; O'Shea, D. F.; Boyle, P. D.; Lindsey, J. S. *J. Org. Chem.* **1999**, *64*, 1391–1396.
29. Farrugia, L. J. *J. Appl. Crystallogr.* **1997**, *30*, 565.